Detection and Quantification of Asymmetric Lipid Vesicle Fusion Using Deuterium NMR†

Carla M. Franzin and Peter M. Macdonald*

Department of Chemistry and Erindale College, University of Toronto, 3359 Mississauga Road, Mississauga, Ontario, Canada, L5L 1C6

Received August 22, 1996; Revised Manuscript Received December 24, 1996⊗

ABSTRACT: It is demonstrated that deuterium nuclear magnetic resonance (^{2}H NMR) spectroscopy can be used to detect and to quantify fusion between anionic giant unilamellar vesicles (GUVs) and cationic small unilamellar vesicles (SUVs). The sensitivity to fusion relies on the conformational response of 1-palmitoyl-2-oleoyl-*sn*-glycero-3-phosphocholine (POPC) to changes in membrane surface electrostatic charge due to lipid mixing upon fusion. This conformational change is reported in the ^{2}H NMR spectrum as a change in the quadrupolar splitting from choline-deuterated POPC. GUVs were composed of varying molar ratios of the anionic lipid 1-palmitoyl-2-oleoyl-*sn*-glycero-3-phosphoglycerol (POPG), plus cholesterol (CHOL), plus POPC. SUVs were composed of the cationic lipid 1,2-dioleoyloxy-3-(dimethylammonio)-propane (DODAP), plus POPC with or without 1-palmitoyl-2-oleoyl-*sn*-glycero-3-phosphoethanolamine (POPE). Using a quantitative model that relates the ^{2}H NMR quadrupolar splitting to the mole fractions of cationic, anionic, and neutral lipids in the vesicle membrane, it was possible to deduce the extent of fusion between the two oppositely-charged vesicle populations directly from the quadrupolar splitting. SUVs composed of DODAP + POPC + POPE (40/40/20) fused 100% with GUVs composed of POPC + CHOL + POPG (60/30/10). Removing POPE from the SUVs reduced the extent of fusion, as did reducing the POPG content of the GUVs.

Membrane fusion is an essential biological process involved in a multitude of cellular activities. These range from intracellular events, such as endocytosis and exocytosis, to various intercellular processes, such as fertilization (Hoekstra, 1990; White, 1992; Wilschut & Hoekstra, 1993). The fusion event itself follows upon the aggregation of two lipid vesicles, and results from a destabilization of the lipid bilayer at the region of vesicle contact and adhesion (Nir *et al.,* 1983). True vesicle fusion results in the simultaneous mixing of the two lipid bilayers and the two aqueous contents of the vesicles involved.

Much of what is known regarding membrane fusion has been gained using liposomes as model systems. The majority of such studies have explored the fusion of lipid vesicles of the same lipid composition. Here, fusion is induced by the addition of fusogenic agents such as Ca^{2+} or polylysine if the vesicles are anionic, and citrate or EDTA if the vesicles are cationic (Portis *et al.,* 1979; Düzgüneş *et al.,* 1989; Ellens *et al.,* 1989; Allen *et al.,* 1990; Helm *et al.,* 1992). In the case of oppositely-charged vesicles, however, fusion occurs spontaneously (Felgner *et al.,* 1987; Stamatatos *et al.,* 1988; Leventis & Silvius, 1990). Fusion studies in general are driven by the need to develop improved drug delivery vehicles, immunodiagnostic applications, and gene therapy techniques (Felgner *et al.,* 1987; Leventis & Silvius, 1990; Litzinger & Huang, 1992; Zhou & Huang, 1994; Wrobel & Collins, 1995; Friend *et al.,* 1996).

Several different techniques for detecting and quantifying vesicle fusion are in common use. These include fluorescence assays that monitor the intermixing of vesicle aqueous contents through fusion-induced changes in the spectroscopic properties of fluorophores trapped within the vesicles (Wilschut *et al.,* 1980; Ellens *et al.,* 1985). A second category of fluorescence assay monitors fusion-induced lipid mixing between the two lipid bilayers by observing the resonance energy transfer between two fluorescent probes covalently attached to different lipids in different vesicles (Struck *et al.,* 1981).

We report here a novel ^{2}H NMR-based technique for detecting and quantifying fusion between oppositely-charged lipid vesicles. When two oppositely-charged vesicles fuse, the mixing of their bilayer lipids changes the surface electrostatic charge of the newly fused vesicle relative to the original donor or acceptor vesicles. The sensitivity of ^{2}H NMR to vesicle fusion arises from the fact that choline-deuterated phosphatidylcholine behaves like a "molecular voltmeter", responding to and, via the ^{2}H NMR spectrum, reporting on lipid bilayer surface electrostatic charge (Akutsu & Seelig, 1981; Seelig & Macdonald, 1987; Scherer & Seelig, 1989; Seelig *et al.,* 1987).

We demonstrate, first, that mixing cationically-charged small unilamellar vesicles (SUVs) with anionically-charged giant unilamellar vesicles (GUVs) containing choline-deuterated phosphatidylcholine produces changes in the ^{2}H NMR spectra consistent with a spontaneous fusion of the SUVs with the GUVs which results in complete mixing of the bilayer lipids of the SUVs and GUVs. Second, we describe how the extent of fusion can be deduced from a simple

† This work was supported by a Graduate Studentship (C.M.F.) and an Operating Grant (P.M.M.) from The National Science and Engineering Research Council of Canada.

* To whom correspondence should be addressed. Telephone: 905-828-3805. Fax: 905-828-5425. E-mail: pmacdona@credit.erin.utoronto.ca.

⊗ Abstract published in *Advance ACS Abstracts,* February 15, 1997.

S0006-2960(96)02127-7 CCC: $14.00

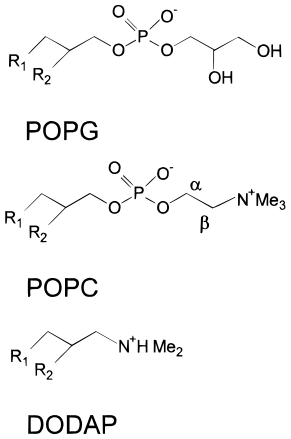

FIGURE 1: Structures of POPG (R_1 = oleoyl acyl chain; R_2 = palmitoyl acyl chain), POPC (R_1 = oleoyl acyl chain; R_2 = palmitoyl acyl chain), and DODAP ($R_1 = R_2$ = oleoyl acyl chain). The designations α and *β* refer to the deutero-labeling positions on the choline group of POPC.

quantitative analysis of the ^{2}H NMR spectra. Finally, we exploit these effects to examine the influence of vesicle surface charge and vesicle lipid composition on the extent of vesicle fusion.

MATERIALS AND METHODS

Materials. Nondeuterated lipids were obtained from Avanti Polar Lipids (Alabaster, AL). Cholesterol (CHOL) was purchased from Fisher (Ottawa, ON) and recrystallized from ethanol prior to use. *n*-Octyl *β*-glucopyranoside (OG), tris(hydroxymethyl)aminomethane (Tris), and oleoyl chloride were obtained from Sigma (St. Louis, MO). Iodomethane, sodium tetraphenylboron, 2,3,4-triisopropylbenzenesulfonyl chloride (TPS), and 3-(dimethylamino)-1,2-propanediol were purchased from Aldrich (Milwaukee, WI). 4-(2-Hydroxyethyl) piperazine-1-ethanesulfonic acid (HEPES) was obtained from BDH (Toronto, ON). 8-Aminonaphthalene-1,3,6-trisulfonic acid, disodium salt (ANTS), and *p*-xylenebis(pyridinium bromide) (DPX) were obtained from Molecular Probes (Eugene, OR).

Synthesis of Choline-Deuterated Phosphatidylcholine. 1-Palmitoyl-2-oleoyl-*sn*-glycero-3-phosphocholine (POPC), selectively deuterated at either the α or the *β* methylene segment, was synthesized by a revision of the methods of Aloy and Rabout (1913) and Harbison and Griffin (1984). Briefly, POPC-α-d_2 and POPC-*β*-d_2 were prepared by coupling the corresponding deuterated choline tetraphenylborate salt to 1-palmitoyl-2-oleoyl-*sn*-glycero-3-phosphate (POPA) in pyridine, using TPS (recrystallized from *n*-pentane) as the condensing agent (Aneja *et al.*, 1970). The structure of the phosphocholine headgroup and the deuteron labeling positions are shown in Figure 1. The deuterated phosphatidylcholines were purified by chromatography on an Amberlite mixed-bed ion exchanger (BDH), followed by precipitation from acetone. The purity of the synthesized lipids was confirmed by thin-layer chromatography and ^{1}H and ^{2}H NMR.

Synthesis of DODAP. 1,2-Dioleoyloxy-3-(dimethylammonio)propane (DODAP) was synthesized as described by Mitrakos and Macdonald (1996) following a modification of the procedure of Leventis and Silvius (1990). The structure of DODAP is shown in Figure 1. Briefly, the acylation of 3-(dimethylamino)-1,2-propanediol with oleoyl chloride was pyridine-catalyzed in dry diethyl ether to yield DODAP. The lipid was purified on a silicic acid column (Rose Scientific Ltd., Edmonton, AL) that was equilibrated with 99/1 (v/v) hexane/acetic acid. The column was eluted consecutively with 20% diethyl ether in hexane, chloroform and 5% methanol in chloroform. Pure DODAP eluted with 5% methanol in chloroform, and was converted to the hydrochloride salt by titration with methanolic HCl prior to use.

S*UV Preparation.* Typically, DODAP, POPE (1-palmitoyl-2-oleoyl-*sn*-glycero-3-phosphoethanolamine), and POPC (all from chloroform stock solutions) were mixed in the desired molar ratios, and the solvent was removed under a stream of nitrogen, followed by overnight desiccation under vacuum. The dried lipids were dispersed in 500 *μ*L of water by vortexing and warming to 40 °C, resulting in the formation of MLVs (multilamellar vesicles). The MLVs were then sonicated 3−5 min using a Braunsonic 1510 sonicator (B. Braun, Melsungen, Germany) equipped with a titanium probe tip. Heating was minimized by immersing the lipid dispersion in ice water. A clear solution was taken as indicative of SUV formation. NaCl buffer (500 *μ*L of 150 mM NaCl, 20 mM HEPES, pH 7.4) was then added to the SUVs (final salt concentration of 75 mM NaCl), and the mixture was resonicated until an opalescent solution was obtained. Finally, the solution was centrifuged to remove metal debris originating from the titanium probe tip.

Preliminary experiments demonstrated that it was not possible to form stable dispersions of cationic SUVs composed of 100% DODAP or DODAP + POPE mixtures at salt concentrations approaching physiological relevance. Rather, such dispersions aggregated within a short time. Stable dispersions of cationic SUVs could be produced at salt concentrations up to approximately 75 mM NaCl when 50 mol % POPC was added to DODAP. When DODAP + POPE mixtures were desired, it was found that stable SUVs could be formed in 75 mM NaCl provided they contained a minimum of 40 mol % POPC and a maximum of 20 mol % POPE.

GUV Preparation. Giant unilamellar vesicles (GUVs) were prepared essentially as described by Marassi *et al.* (1993). Typically, deuterated POPC (20 mg) was mixed with the desired molar ratio of POPG (1-palmitoyl-2-oleoyl-*sn*-glycero-3-phosphoglycerol) and cholesterol (CHOL) by mixing the requisite volumes of chloroform stock solutions of the individual lipids. The solvent was removed under a stream of nitrogen gas followed by vacuum desiccation overnight. The dried lipids were dispersed in approximately 750 *μ*L of NaCl buffer (typically 75 mM NaCl, 10 mM HEPES, pH 7.4) plus OG in a detergent/lipid molar ratio of 12/1. The mixture was vortexed and warmed to 40 °C until a transparent solution formed (generally virtually immediately). The detergent/lipid mixture was injected into the dialysis cell of a MiniLipoPrep dialyzer (Avestin, Ottawa, ON) and dialyzed through a cellulose membrane (molecular weight cutoff 5000; Diachema, Switzerland) against 1 L of NaCl buffer. Dialysis proceeded for 48 h, with four buffer changes.

Mixing of GUVs and SUVs. The desired increment of SUVs was added slowly to the GUV dispersion with gentle mixing. The SUV + GUV mixture was then concentrated using a Centricon-30 microconcentrator (Amicon, Oakville, ON), and the concentrated vesicular dispersion was trans-

ferred directly to an NMR sample holder for NMR spectroscopy. Further incremental additions of SUVs were made to a given SUV + GUV mixture by the same procedure with a concentration step after each addition.

NMR Measurements. ^{2}H NMR spectra of vesicle samples were recorded on a Chemagnetics CMX300 NMR spectrometer operating at 45.98 MHz, using a Chemagnetics broadline deuterium probe equipped with a 10 mm diameter solenoid coil. The quadrupolar echo pulse sequence [90_x-t-90_y-t-acq] (Davis *et al.*, 1976) was employed using quadrature detection with complete phase cycling of the pulse pairs. The 90° pulse length was 11 μs, the interpulse delay was 40 μs, the recycle delay was 100 ms, the spectral width was 100 kHz, and the data size was 2K. All spectra were recorded at room temperature.

^{31}P NMR spectra were recorded on the same spectrometer operating at 121.25 MHz, using a Chemagnetics double-resonance magic angle spinning probe but without sample spinning. The Hahn echo sequence [$90_x-t-180_y-t-$acq] with complete phase cycling of the pulses and proton decoupling during acquisition was employed as described by Rance and Byrd (1983). The 90° pulse length was 5 μs, the echo-spacing was 40 μs, the recycle delay was 3 s, the spectral width was 100 kHz, and the data size was 2K. All spectra were recorded at room temperature.

Fluorescence Fusion Assays. Aqueous content mixing upon vesicle fusion was determined independently using the ANTS/DPX assay described by Ellens *et al.*, (1985). In this fusion assay, DPX-encapsulated SUVs are added to ANTS-encapsulated GUVs, and the mixing of their aqueous contents upon fusion is manifested as a decrease in ANTS fluorescence due to its quenching by DPX. DPX quenches ANTS fluorescence by classical Förster energy transfer, and the quenching is DPX concentration dependent (Ellens *et al.*, 1985). GUVs of composition POPC + CHOL + POPG (60/20/20) were first prepared in 20 mM NaCl (10 mM Tris, pH 7.4) and then loaded with 12.5 mM ANTS by freeze-fracturing a 400 μL aliquot of GUVs (~8 μmol of lipid) with 400 μL of 25 mM ANTS, 20 mM NaCl (10 mM Tris, pH 7.4). ANTS was removed from the external GUV solution by passing the vesicles through a 30 mL Sephadex-G10 column (Sigma, St. Louis, MO) equilibrated in 50 mM NaCl (10 mM Tris, pH 7.4). SUVs of composition POPC + DODAP (50/50) or POPC + DODAP + POPE (40/40/20) were preformed by sonication in 700 μL of water and then loaded with 45 mM DPX (10 mM Tris, pH 7.4) by addition of 700 μL of 90 mM DPX (20 mM Tris, pH 7.4) followed by sonication. DPX was removed from the external SUV solution by passing the vesicles through a 20 mL Sephadex-G10 column equilibrated in 50 mM NaCl (10 mM Tris, pH 7.4).

Leakage of vesicle contents upon fusion was monitored by a related ANTS/DPX assay, following a procedure described by Ellens *et al.* 1985. In this assay, GUVs with entrapped ANTS + DPX exhibit no ANTS fluorescence due to DPX quenching. Upon leakage of the vesicle contents, ANTS fluorescence increases due to a dilution of DPX into the surrounding medium. Hence, leakage due to fusion is monitored as an increase in the ANTS fluorescence upon additions of SUVs. GUVs of composition POPC + CHOL + POPG (60/20/20) were first prepared in 20 mM NaCl (10 mM Tris, pH 7.4) and then loaded with 6.25 mM ANTS, 22.5 mM DPX, and 10 mM NaCl (10 mM Tris, pH 7.4) by freeze-fracturing a 400 μL aliquot of GUVs (~8 μmol of lipid) with 400 μL of 12.5 mM ANTS, 45 mM DPX (10 mM Tris, pH 7.4). ANTS and DPX were removed from the external GUV solution by passing the vesicles through a Sephadex-G10 column equilibrated in 50 mM NaCl (10 mM Tris, pH 7.4). SUVs of the same composition as described above were formed by sonication in 1.4 mL of 50 mM NaCl (10 mM Tris, pH 7.4).

In both the aqueous content mixing and the leakage assays, ANTS fluorescence was measured using an SLM 4800 spectrofluorometer (excitation, 380 nm; emission, 510 nm). Typically, the assay was carried out with total GUV lipid concentrations up to 100 μM. Triton X-100 [octylphenoxypoly(ethoxyethanol); Sigma] was used to lyse the vesicles at the end of each assay.

RESULTS AND DISCUSSION

^{2}H NMR Detection of the Fusion of Cationic SUVs with Anionic GUVs. Figure 2 shows a series of ^{2}H NMR spectra obtained with anionic GUVs composed of POPC + CHOL + POPG (60/30/10) and containing either POPC-α-d_2 (left-hand spectra) or POPC-β-d_2 (right-hand spectra). The top spectra in both cases were obtained in the absence of added SUVs. In both instances, the ^{2}H NMR spectral line shape consists of a motionally-narrowed Pake-doublet powder pattern. This line shape is typical of lipids in a liquid-crystalline bilayer where they undergo rapid anisotropic motional averaging about their long molecular axes, but only slow isotropic motional averaging from the combined effects of overall vesicle tumbling and lipid lateral diffusion within the bilayer plane. Provided that the GUVs have a diameter greater than approximately 500 nm, the correlation time for vesicle tumbling and lipid lateral lipid diffusion will be slow on the ^{2}H NMR time scale (Bloom *et al.*, 1975). GUVs of the composition used here have diameters on the order of 800 nm and, therefore, display no deleterious vesicle size effects (Marassi *et al.*, 1993). The quadrupolar splitting ($\Delta\nu_Q$) corresponds to the separation, in hertz, between the two maxima or "horns" in such spectra. The presence of 10 mol % POPG is manifested in such spectra by the fact that the quadrupolar splitting for the GUVs containing POPC-α-d_2 increases relative to control values, while the quadrupolar splitting for the GUVs containing POPC-β-d_2 decreases relative to control values. This counter-directional change in the size of the quadrupolar splittings from POPC-α-d_2 versus POPC-β-d_2 is indicative of a conformational change undergone by the choline headgroup of POPC in response to the presence of surface charges (Seelig & Macdonald, 1987; Seelig *et al.*, 1987; Scherer & Seelig, 1989). In this instance, the ^{2}H NMR response is consistent with the accumulation of negative charges at the lipid bilayer surface of the vesicles. Since only a single quadrupolar splitting is observed, one concludes that both the inner and outer monolayer surfaces of the lipid bilayers experience identical surface charge densities. Indeed, under these circumstances, no transmembrane surface charge asymmetries are to be expected. As shown previously, cholesterol has little or no effect on the ^{2}H NMR spectra of choline-deuterated POPC (Marassi *et al.*, 1993).

The narrow resonance at 0 Hz in the ^{2}H NMR spectra arises from the natural abundance deuterium in water, HDO, rather than from any isotropically-averaging lipid population.

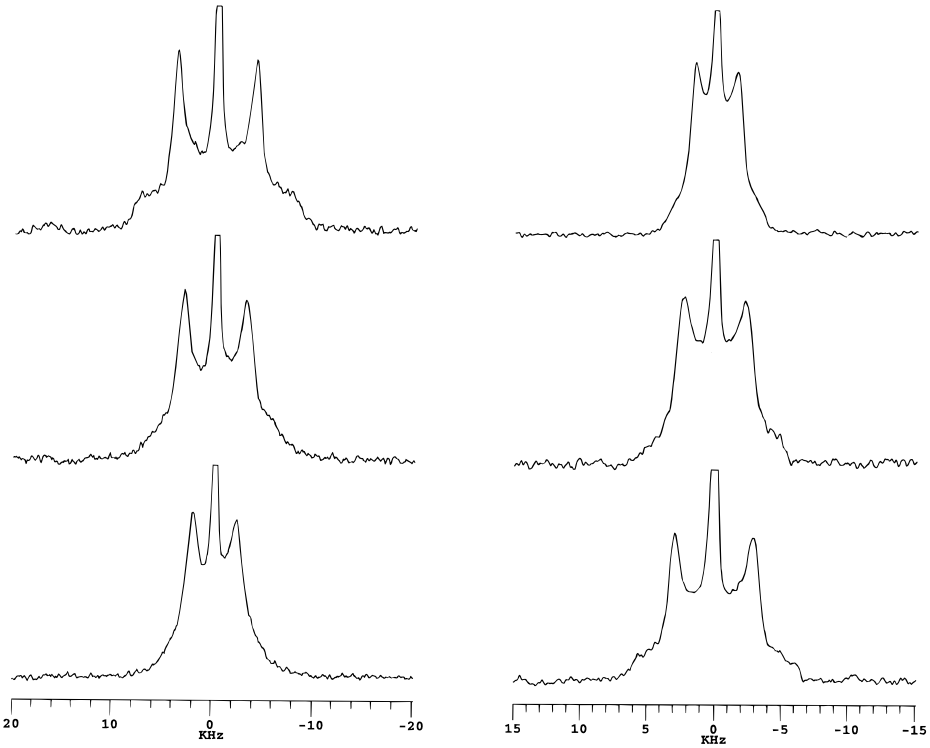

FIGURE 2: ^{2}H NMR spectra of GUVs composed of POPC + CHOL + POPG (60/30/10) as a function of added SUVs composed of DODAP + POPC (50/50). Spectra for POPC-α-d_2 are shown on the left, while spectra from POPC-β-d_2 are shown on the right. Top spectra: GUVs with no SUVs added. Middle spectra: GUVs with SUVs added in a ratio of 0.174 SUV lipid per GUV lipid. Bottom spectra: GUVs with SUVs added in a ratio of 0.521 SUV lipid per GUV lipid. All spectra were recorded at room temperature.

The ^{31}P NMR spectra to be presented below confirm the absence of any isotropic lipid in the controls. The recycle delay of 100 ms used in acquiring these spectra largely suppresses the HDO resonance, but the dilute nature of the GUV preparations means that a significant contribution from HDO remains.

The middle and bottom ^{2}H NMR spectra in Figure 2 depict the effects of adding cationic SUVs composed of DODAP + POPC (50/50) to the same anionic GUVs. The middle spectra correspond to the case that the global DODAP/POPG ratio in the SUV/GUV mixture equals approximately 0.87. In the bottom spectra, the global DODAP/POPG ratio equals approximately 2.60. For the case of anionic GUVs containing POPC-α-d_2, the addition of cationic SUVs causes the quadrupolar splitting to decrease. When the anionic GUVs contain POPC-β-d_2, the quadrupolar splitting increases when cationic SUVs are added. Again, this counter-directional change in the size of the quadrupolar splittings from POPC-α-d_2 versus POPC-β-d_2 is characteristic of the "molecular voltmeter" response to changes in lipid bilayer surface charge. In this instance, the direction of the change indicates that the cationic charge from the SUVs is neutralizing the anionic charge at the membrane surface of the GUVs. In each spectrum in Figure 2, only a single quadrupolar splitting can be resolved, indicating that both the inner and the outer leaflet of the GUV bilayer experiences an identical change in surface charge density upon adding SUVs.

Figure 3 is a plot of the size of the quadrupolar splitting measured from the ^{2}H NMR spectra of POPC-α-d_2 and POPC-β-d_2 incorporated into GUVs composed of POPC + CHOL + POPG (60/30/10) as a function of progressive incremental additions of SUVs composed of DODAP + POPC (50/50). Successive SUV additions produce further changes in the quadrupolar splitting from both POPC-α-d_2 and POPC-β-d_2. The dependence on the DODAP/POPG charge ratio is approximately linear at both deutero-labeling positions, at least to the limits plotted in Figure 3. The counter-directional change in the size of the quadrupolar splitting, which is characteristic of the specific conformational response of the choline headgroup of POPC to the presence of surface charge, is particularly evident. Furthermore, it is clear that POPC-α-d_2 is much more sensitive to the presence of DODAP than is POPC-β-d_2. This is consistent with the ^{2}H NMR calibration measurements on related lipid mixtures in MLVs reported by Mitrakos and Macdonald (1996). The quadrupolar splittings from these

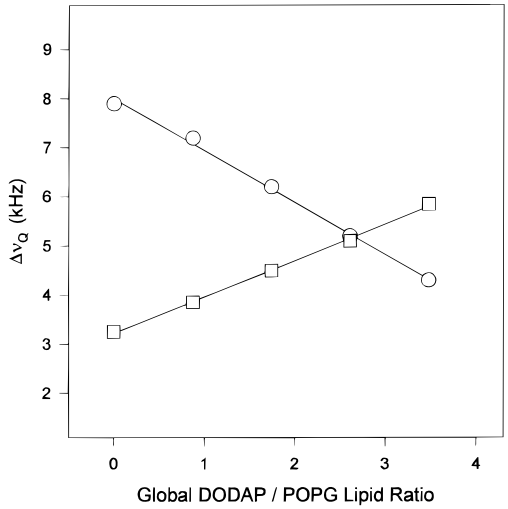

FIGURE 3: ^{2}H NMR quadrupolar splittings from POPC-α-d_2 (circles) and POPC-β-d_2 (squares) incorporated into GUVs composed of POPC + CHOL + POPG (60/30/10) as a function of added SUVs composed of DODAP + POPC (50/50).

Table 1: Experimental ^{2}H NMR Quadrupolar Splittings for GUVs Mixed with SUVs

vesicle lipid composition	global SUV/ GUV lipid ratio	global DODAP/ POPG lipid ratio	$\Delta\nu_Q$ (kHz) POPC-α-d_2	$\Delta\nu_Q$ (kHz) POPC-β-d_2
GUV POPC/CHOL/POPG (60/30/10) + SUV DODAP/POPC (50/50)	0	0	7.9	3.3
	0.174	0.87	7.2	3.9
	0.347	1.7	6.2	4.5
	0.521	2.6	5.2	5.1
	0.695	3.5	4.3	5.9
GUV POPC/CHOL/POPG (70/20/10) + SUV DODAP/POPC (50/50)	0	0	7.6	3.5
	0.203	1.0	6.9	3.9
	0.405	2.0	5.8	4.5
	0.608	3.0	5.0	5.0
	0.812	4.0	4.3	5.5
GUV POPC/CHOL/POPG (69/30/1) + SUV DODAP/POPC (50/50)	0	0	6.3	
	0.200	10	6.2	
	0.400	20	5.9	
	0.600	30	5.3	
	1.00	40	4.5	
GUV POPC/CHOL/POPG (60/30/10) + SUV DODAP/POPC/POPE (40/40/20)	0	0	7.4	
	0.109	0.44	6.5	
	0.217	0.87	5.7	
	0.326	1.3	5.1	
	0.434	1.7	4.8	
	0.543	2.2	4.5	
	0.651	2.6	4.0	

and other measurements described here are reported in Table 1.

A logical explanation for the effects on the ^{2}H NMR spectra of adding cationic SUVs to anionic GUVs is that fusion of the SUVs with the GUVs has led to mixing of the SUV cationic lipids with the GUV anionic lipids. Possible interactions other than fusion do not, in general, predict the same observations. Spontaneous lipid transfer, for instance, is too slow to account for the immediacy of the observed effects. Furthermore, if the cationic SUVs were simply binding electrostatically to the outer monolayer of the GUVs, then the inner and the outer leaflets of a GUV lipid bilayer should have different surface charge densities. One would expect, therefore, to observe two quadrupolar splittings were this the case. Likewise, if fusion were only occurring between the outer leaflets of the SUV and GUV bilayers in a type of lipid transfer event (such as hemifusion), then two quadrupolar splittings should be evident, given that rates of transbilayer lipid flip-flop are expected to be slow on the time scale of the ^{2}H NMR measurements. It is also important to note that the GUV + SUV mixtures were concentrated by centrifugation prior to obtaining the NMR spectrum. It is possible that centrifugation induces fusion through its concentrating effect. To eliminate the possibility that centrifugation induced fusion, ^{2}H NMR spectra of GUV + SUV mixtures were acquired without any concentrating step. In these instances, the ^{2}H NMR spectra were again characteristic of fusion, with quadrupolar splittings comparable to those obtained with the centrifugation−concentration step (data not shown).

It is necessary to assess at this point whether intact bilayers remain after the fusion event. Our ^{2}H NMR spectra show no indication of any nonbilayer phases. ^{31}P NMR, however, provides a more definitive analysis of the macroscopic phase state of self-assembled phospholipids, and readily differentiates bilayer versus hexagonal H_{II} versus isotropic or cubic phospholipid phases (Seelig, 1978; Cullis & de Kruijff, 1979). Figure 4 shows a series of ^{31}P NMR spectra for anionic GUVs of various composition in the presence of various added cationic SUVs. The top ^{31}P NMR spectrum in Figure 4 was obtained with GUVs composed of POPC + CHOL + POPG (60/30/10). The spectral line shape is characteristic of phospholipids in a liquid-crystalline bilayer arrangement. The residual chemical shift anisotropy, $\Delta\sigma$,

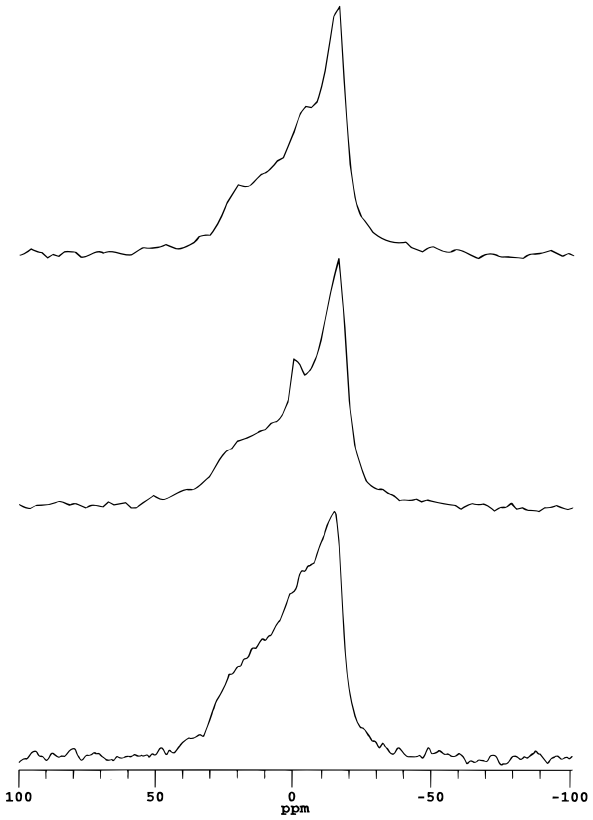

FIGURE 4: ^{31}P NMR spectra of GUVs composed of POPC + CHOL + POPG (60/30/10). Top spectrum: GUVs with no SUVs added. Middle spectrum: GUVs with SUVs of composition DODAP + POPC (50/50) in an amount equal to 0.521 SUV lipid per GUV lipid. Bottom spectrum: GUVs with SUVs of composition POPC + DODAP + POPE (40/40/20) in an amount equal to 0.651 SUV lipid per GUV lipid. All spectra were recorded at room temperature.

corresponding to the frequency separation between the two shoulders in the spectrum, equals 41 ppm, in agreement with previously reported values for such GUVs (Marassi *et al.*, 1993). The middle spectrum represents the same GUVs in the presence of SUVs composed of DODAP + POPC (50/50) in an amount yielding a global DODAP/POPG ratio of 2.6. It is evident that the overall spectral line shape and $\Delta\sigma$ are almost unchanged relative to the GUVs alone. The presence of phospholipid in a hexagonal H_{II} phase would be manifested in the ^{31}P NMR spectra by a component having $\Delta\sigma$ decreased by half and reversed in sign. A small isotropic resonance is visible, representing excess, unfused SUVs. We note that under the spectral acquisition conditions used here the intensity ratio of the bilayer spectral component versus the isotropic spectral component cannot be used to quantify reliably the relative amounts of phospholipid in the two environments since the resonance of the small, isotropically-tumbling SUVs will be partially saturated.

It is believed that asymmetric fusion, i.e., fusion between anionic and cationic liposomes, occurs due to electrostatic attraction which leads to vesicle aggregation, partial surface charge neutralization, and dehydration of the polar headgroups. This results, in turn, in the formation of molecular packing defects which act as nucleation sites for membrane and aqueous content intermixing. This is similar to the mechanism by which divalent cations such as Ca^{2+} and Ba^{2+} are thought to induce symmetric fusion, i.e., fusion between like vesicles, in anionic liposomes. It is believed, however, that the presence of complementary fixed surface charges on two asymmetric lipid vesicles can promote interactions between the vesicles with greater efficiency than can a neutralization of charge repulsion between vesicles by divalent ions (Stamatatos *et al.*, 1988).

We investigated the influence of surface charge density on fusion in our system by mixing cationic SUVs composed of DODAP + POPC (50/50) with anionic GUVs of the general composition POPC + CHOL + POPG [(70 − *x*)/30/*x*] having various amounts of POPG. Figure 5 shows the resulting quadrupolar splittings for POPC-α-d_2 plotted as the difference, $\Delta\nu_Q^{diff}$, between the measured splitting before and after SUV addition. Cationic SUVs added to GUVs composed of POPC + CHOL (70/30), i.e., in the absence of POPG, exhibited no fusion as indicated by the lack of change in the quadrupolar splitting. This is consistent with the requirement for the presence of complementary surface charges on the two vesicle populations. GUVs composed of POPC + CHOL + POPG (69/30/1) exhibited a detectable level of fusion, but rather high amounts of SUVs were required to produce an observable effect. GUVs composed of POPC + CHOL + POPG (60/30/10) exhibited an almost linear change in the quadrupolar splitting with amount of added SUVs. These results demonstrate the essential role of the GUV membrane surface charge as an inducer of fusion with the SUVs. Since only a single quadrupolar splitting was observed in every case, these results further indicate that there is no intermediate situation in which the SUVs simply bind to the GUVs surface, or mix only with the GUVs outer monolayer, but do not fuse completely.

It is in fact somewhat surprising that fusion occurs in these systems in the absence of a fusogenic agent such as phosphatidylethanolamine. It is possible that the cholesterol in our GUVs might be promoting fusion (Yeagle, 1988).

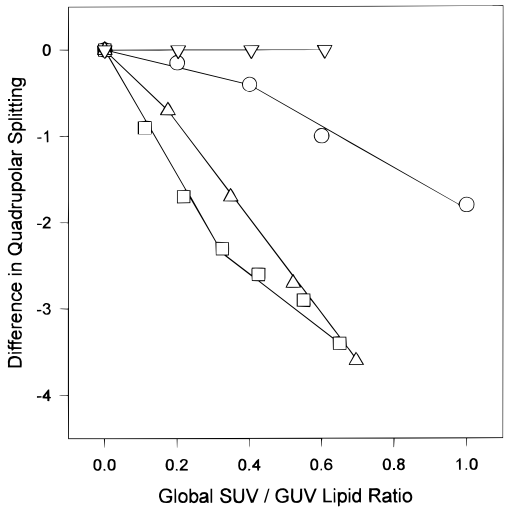

FIGURE 5: ^{2}H NMR quadrupolar splittings from POPC-α-d_2 incorporated into GUVs of various composition as a function of added SUVs. Inverted triangles: GUVs = POPC + CHOL (70/30), SUVs = DODAP + POPC (50/50). Circles: GUVs = POPC + CHOL + POPG (69/30/1), SUVs = DODAP + POPC (50/50). Triangles: GUVs = POPC + CHOL + POPG (60/30/10), SUVs = DODAP + POPC (50/50). Squares: GUVs = POPC + CHOL + POPG (60/30/10), SUVs = DODAP + POPC + POPE (40/40/20). The solid lines represent the average extent of fusion, determined according to eq 6 for a given range of global SUV/GUV lipid ratios, as described in the text.

Cholesterol might change the spacing between the POPG headgroups, thereby altering the coordination geometry of the cationic SUV/anionic GUV complex. Alternatively, the particular complex formed in the presence of cholesterol may lead to sufficient dehydration at the region of contact between the membranes to mediate fusion.

When ^{2}H NMR was used to detect fusion between cationic SUVs composed of DODAP + POPC (50/50) and anionic GUVs composed of POPC + CHOL + POPG (either 70/20/10 or 60/30/10), there was no discernible difference in the response of the quadrupolar splittings. The results are listed in Table 1. Unfortunately, it is not possible for us to explore a much wider range of cholesterol concentrations, since lower concentrations produce smaller GUVs and limit our ability to perform the ^{2}H NMR analysis.

A detailed quantitation of the extent of fusion as extracted from the ^{2}H NMR data will be presented below. At this point, we would note that a simple comparison indicates that for these liposome compositions only a fraction of the SUVs added are actually fusing with the GUVs. Specifically, the quadrupolar splittings for GUVs composed of POPC + CHOL + POPG (60/30/10) were 7.2 and 3.85 kHz for POPC-α-d_2 and POPC-β-d_2, respectively, after adding sufficient SUVs composed of DODAP + POPC (50/50) such that the DODAP/POPG ratio was 0.87. These values are significantly reduced relative to controls, indicating that some fusion has occurred. However, an MLV dispersion having the same global lipid composition, i.e., POPC + CHOL + POPG + DODAP (68.7/30/10/8.7), yields quadrupolar splittings that are much further reduced relative to the GUV + SUV mixture: specifically, 5.5 kHz for POPC-α-d_2 and 5.4 kHz for POPC-β-d_2. Therefore, not all SUVs added have fused with GUVs.

Enhancement of Fusion by Phosphatidylethanolamine. Phosphatidylethanolamine (PE) is a highly fusogenic lipid because it has a small surface hydration, which encourages

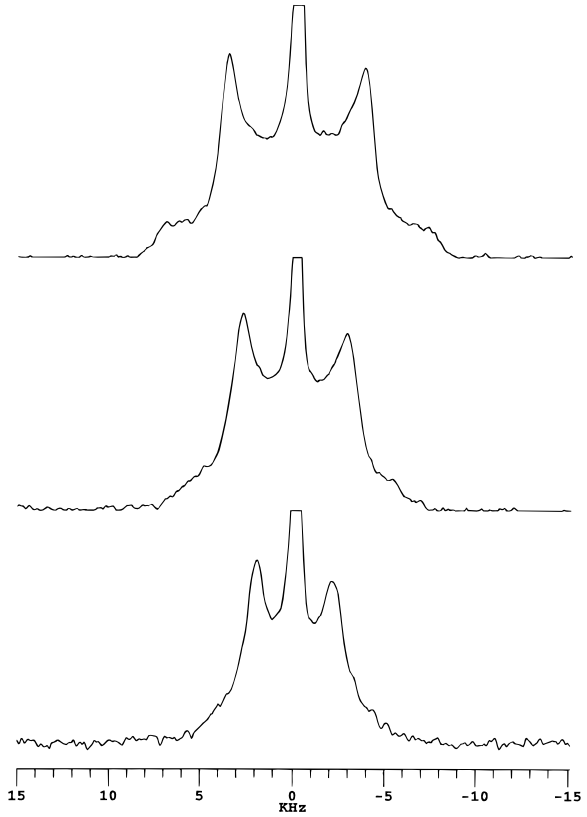

FIGURE 6: ^{2}H NMR spectra for GUVs composed of POPC-α-d_2 + CHOL + POPG as a function of added SUVs of composition DODAP + POPC + POPE (40/40/20). Top spectrum: GUVs with no SUVs added. Middle spectrum: GUVs with SUVs added in a ratio of 0.217 SUV lipid per GUV lipid. Bottom spectrum: GUVs with SUVs added in a ratio of 0.651 SUV lipid per GUV lipid. All spectra were recorded at room temperature.

the close apposition of two membrane surfaces. PE can associate and mix with phosphatidylcholine-rich membranes, and it has been found that it need only be present in one of the fusing vesicles to have a positive effect on fusion (Wrobel & Collins, 1995). For these reasons, PE-containing vesicles are used in DNA transfection systems. Furthermore, PE-containing cationic vesicles form more compact complexes with DNA than their phosphatidylcholine counterparts, and this appears to increase DNA transfection efficiency (Gustaffson *et al.,* 1995).

Figure 6 shows a series of ^{2}H NMR spectra of GUVs composed of POPC-α-d_2 + CHOL + POPG (60/30/10) to which have been added SUVs composed of DODAP + POPC + POPE (40/40/20). The control ^{2}H NMR spectrum for the GUVs in the absence of added SUVs is again shown at the top. The DODAP/POPG ratio due to added SUVs in the middle and bottom spectra again equals 0.87 and 2.6, respectively. After the first addition of SUVs, the GUV quadrupolar splitting decreases a total of 1.75 kHz from the control value. This is a much greater change than that obtained for an equivalent DODAP/POPG ratio for SUVs lacking POPE, suggesting a greater extent of fusion in the presence of POPE. The trend continues when further increments of SUVs are added, as shown by the bottom spectrum. Once again, the quadrupolar splitting decreases from the control value, and the net change is greater than that obtained for an equivalent DODAP/POPG ratio for SUVs lacking POPE.

Returning to Figure 5, one can compare the effects of adding cationic SUVs with and without POPE on the quadrupolar splittings from GUVs composed of POPC-α-d_2 + CHOL + POPG (60/30/10). The quadrupolar splittings are plotted as the difference, $\Delta\nu_Q^{diff}$, relative to the control value prior to SUV addition. For cationic SUVs lacking POPE, the quadrupolar splitting decreases almost linearly. For SUVs containing POPE, the quadrupolar splitting decreases sharply until the global DODAP/POPG ratio equals approximately 1.0, and thereafter continues to decrease albeit with a lesser slope.

A simple comparison demonstrates that the POPE-containing cationic SUVs fuse almost quantitatively with the anionic GUVs. Specifically, the measured quadrupolar splitting from POPC-α-d_2 was 5.65 kHz upon adding sufficient POPE-containing SUVs to achieve a global DODAP/POPG ratio of 0.87. When an MLV dispersion of the identical global lipid composition was prepared, i.e., POPC + CHOL + POPG + DODAP + POPE (68.7/30/10/8.7/4.35), the quadrupolar splitting from POPC-α-d_2 was measured to be 5.5 kHz, virtually identical to the corresponding GUV + SUV mixture. This indicates that complete mixing of the GUV lipids with all the added SUV lipids has occurred, and this is only possible through vesicle fusion.

The ^{2}H NMR line shapes of the spectra in Figure 6 are comparable to those in Figure 2 in that they are typical of lipids in a liquid-crystalline bilayer. Therefore, the amount of POPE present in the fused GUVs is insufficient to cause any conversion to a nonbilayer lipid phase. The fact that one observes only a single quadrupolar splitting indicates that there is only one lipid population experiencing the same overall net surface charge. These interpretations are confirmed by the ^{31}P NMR spectra of the anionic GUVs fused with POPE-containing cationic SUVs shown at the bottom of Figure 4. The line shape of this ^{31}P NMR spectrum is typical of bilayer lipids overall. However, there is some rounding of the shoulders in the spectrum as well as a decrease in the chemical shift anisotropy ($\Delta\sigma$).

This finding that the lipids retain a bilayer arrangement post-fusion, even when POPE is present, is significant. It has been observed that there is a strong correlation between the tendency of vesicles to fuse and the propensity of the component lipids to adopt nonbilayer phases, such as the H_{II} organization, particularly when PE is involved (Ellens *et al.,* 1989; Bailey & Cullis, 1994). It has also been reported, however, that at lower concentrations of phospholipids, and at temperatures where the lipids remain in the lamellar state, vesicles containing PE can be made to aggregate and fuse without the leakage of contents that normally results during the formation of the H_{II} phase (Allen *et al.,* 1990). This is important in cases where a system is being developed for drug delivery or DNA transfection. One desires the vesicles to interact with the host cell or liposome and to transfer their contents, but not to lyse the cell or otherwise cause leakage of the contents. The permeability barrier may be compromised if there is a conversion from a bilayer to an inverted hexagonal (H_{II}) lipid phase, or if there is a collapse to smaller cochleate (spiral) structures [see Ellens *et al.* (1985) and references cited therein]. Our results reported here indicate that if any H_{II} phase forms during the fusion of such asymmetric vesicles, it is either too transient or too small an amount to be detected by either ^{2}H or ^{31}P NMR.

Table 2: Fluorescence Assay of Aqueous Contents Mixing upon GUV−SUV Fusion

solution compositions, GUV POPC/CHOL/POPG (60/20/20) + 12.5 mM ANTS[a]	global SUV/GUV lipid ratio	global DODAP/POPG lipid ratio	% max ANTS fluorescence
60 μM GUV lipid	0	0	100
+0.05 wt % Triton	0	0	100
+1.55 mM DPX	0	0	92
+3.00 mM DPX	0	0	90
+0.05 wt % Triton X-100 + 3.00 mM DPX	0	0	0
100 μM GUV lipid	0	0	100
+SUV (DODAP/POPC/POPE, 40/40/20)	3.30	7.0	100
+SUV + 0.05 wt % Triton X-100	3.30	7.0	0
+SUV (DODAP/POPC, 50/50)	2.63	7.0	100
+SUV + 0.05 wt % Triton X-100	2.63	7.0	0

[a] 12.5 mM ANTS is the concentration trapped within the GUVs.

Table 3: Fluorescence Assay of Vesicle Contents Leakage upon GUV−SUV Fusion

solution compositions, GUV[b] POPC/CHOL/POPG (60/20/20) + 6.25 mM ANTS + 22.5 mM DPX	global SUV/GUV lipid ratio	global DODAP/POPG lipid ratio	% max ANTS fluorescence[a]
60 μM GUV lipid	0	0	0
+SUV (DODAP/POPC/POPE, 40/40/20)	1.27	3.0	0
+SUV (DODAP/POPC/POPE, 40/40/20)	2.52	5.0	0
+SUV (DODAP/POPC/POPE, 40/40/20)	3.75	8.0	3
+SUV (DODAP/POPC/POPE, 40/40/20)	6.12	13.0	33
+0.05 wt % Triton X-100	6.12	13.0	100
+SUV (DODAP/POPC, 50/50)	4.88	13.0	20
+0.05 wt % Triton X-100	4.88	13.0	100
110 μM GUV lipid	0	0	0
+SUV (DODAP/POPC/POPE, 40/40/20)	3.26	7.0	30
+0.05 wt % Triton X-100	3.26	7.0	100
+SUV (DODAP/POPC, 50/50)	2.60	7.0	16
+0.05 wt % Triton X-100	2.60	7.0	100

[a] Fluorescence intensity at 30 min post-SUV addition. [b] GUVs contain both ANTS and DPX entrapped in concentrations of 6.25 mM and 22.5 mM, respectively.

Fluorescence Assay of Vesicle Contents Mixing and Leakage upon Fusion. To demonstrate via an independent method that fusion occurs in these systems, we employed the ANTS/DPX fluorescence assay described by Ellens *et al*. (1985). In order to measure aqueous content mixing, DPX-loaded cationic SUVs (internal DPX concentration of 45 mM) are added to ANTS-loaded anionic GUVs (internal ANTS concentration of 12.5 mM), and the ANTS fluorescence intensity is monitored as described under Materials and Methods. The fluorescence results are listed in Table 2. First, in order to demonstrate that ANTS is present exclusively in the GUV interior and absent from the exterior solution, one attempts to quench its fluorescence by simply adding DPX to the exterior solution. As shown in Table 2, even after adding 3.0 mM DPX, 90% of the initial ANTS fluorescence remains. Thus, the bulk of the ANTS present in the cuvette is entrapped within GUVs and protected from externally added DPX. However, if the GUVs are lysed by adding Triton detergent, 3.0 mM DPX quenches the ANTS fluorescence entirely. If Triton is added to the GUVs with entrapped ANTS without adding DPX, the fluorescence intensity is unchanged. Thus, there is neither self-quenching nor inner filter effects influencing the ANTS fluorescence at the concentrations employed here.

When DPX-loaded cationic SUVs are added to ANTS-loaded anionic GUVs, there is no change in the ANTS fluorescence intensity, again as shown in Table 3. The same result is obtained regardless of whether or not POPE is present in the SUV lipids. This result would seem to indicate that no mixing of the internal vesicle contents, and hence no fusion, has occurred. However, from such data one cannot conclude that fusion has not occurred. It is entirely possible that vesicle fusion and mixing of the vesicles' aqueous contents occur, only to be followed virtually immediately by leakage (Stamatatos *et al.*, 1988). The effect of leakage of vesicle contents is to dilute the DPX concentration to the extent that it is no longer capable of quenching the ANTS fluorescence. This would be on a time scale too short to be monitored using our fluorescence measurements.

To demonstrate definitively that leakage of vesicle contents occurs when our cationic SUVs are added to anionic GUVs, one entraps both ANTS and the quencher DPX within the GUVs and monitors the ANTS fluorescence upon adding SUVs. Vesicle fusion accompanied by leakage of aqueous contents should produce an increased ANTS fluorescence as DPX is diluted into the exterior solution. Prior to the addition of SUVs, as shown in Table 3, the ANTS fluorescence is entirely quenched due to the high DPX concentration in the interior of the GUVs (Ellens *et al.*, 1984). Adding cationic SUVs to the anionic GUVs with entrapped ANTS + DPX causes the ANTS fluorescence to increase, indicating that leakage of vesicle contents occurs. The maximum ANTS fluorescence is observed upon lysis of the vesicles with Triton detergent. One observes, from the data in Table 3, that the presence of POPE enhances leakage, as expected given its fusogenic properties. However, the DODAP/POPG ratios required to achieve an observable change in fluorescence intensity are much greater than those producing the effects observed via ^{2}H NMR. A major difference between the fluorescence and the ^{2}H NMR experiments is the total

vesicle lipid concentration, which is approximately a factor of 1000 higher in the NMR sample holder versus the fluorescence cuvette. It is simply not possible to perform fluorescence intensity measurements at the lipid concentrations essential for the NMR measurements. One expects that the overall vesicle concentration will be a significant factor in deciding the degree of fusion, since aggregation is an important initial step in the fusion. Indeed, as shown in Table 3, when the GUV concentration is approximately doubled, the DODAP/POPG ratio required to achieve a comparable fluorescence increase upon SUV addition is approximately halved.

To summarize, our fluorescence assays confirm that leakage of vesicle contents occurs upon adding cationic SUVs to anionic GUVs, implying, but not proving definitively, that vesicle fusion occurs. However, leakage of aqueous contents is commonly observed to accompany vesicle fusion (Stamatatos *et al.*, 1988; and references cited therein). In the experimental design employed here, the ^{2}H NMR technique provides information regarding lipid mixing between the SUV and GUV lipids, but not about mixing or leakage of aqueous vesicle contents. However, the ^{2}H and ^{31}P NMR results do reveal that intact bilayers remain following mixing of GUVs with SUVs, and this rules out the possibility that leakage of aqueous contents is due to the formation of nonbilayer phases. Therefore, membrane fusion and mixing of aqueous contents followed by leakage remains the best explanation for the combined NMR and fluorescence results.

Quantifying the Extent of Vesicle Fusion from ^{2}H NMR Data. We have shown that ^{2}H NMR of choline-deuterated POPC can be used to detect fusion between cationic SUVs and anionic GUVs via the changes that fusion induces in the GUV's lipid bilayer surface charge density. In the following section, we describe how to extract information regarding the extent of vesicle fusion from the ^{2}H NMR quadrupolar splittings.

The ^{2}H NMR quadrupolar splittings of POPC-α-d_2 and POPC-β-d_2 depend sensitively on the content of charged lipids in the lipid bilayer. For binary mixtures of POPC plus either a cationic or an anionic amphiphile, the quadrupolar splittings depend in an approximately linear fashion on the mole fraction of cationic (X_+) or anionic (X_-) amphiphile as described by eq 1:

$$\Delta\nu_- = m_-X_- + \Delta\nu_0 \qquad (1)$$

$$\Delta\nu_+ = m_+X_+ + \Delta\nu_0$$

where $\Delta\nu_+$ and $\Delta\nu_-$ refer to the quadrupolar splitting measured in the presence of either cationic or anionic amphiphiles, $\Delta\nu_0$ is the quadrupolar splitting measured with 100% POPC bilayers, and m_+ and m_- are proportionality constants measured in separate calibration experiments. For DODAP, m_+ equals −21.2 kHz/mol and +11.6 kHz/mol for POPC-α-d_2 and POPC-β-d_2, respectively (Mitrakos & Macdonald, 1996). For POPG, m_- equals +9.6 kHz/mol and −8.4 kHz/mol for POPC-α-d_2 and POPC-β-d_2, respectively (Macdonald *et al.*, 1991).

For ternary mixtures of POPC with both cationic and anionic amphiphiles, the observed quadrupolar splitting, $\Delta\nu_{+/-}$, is perturbed relative to the value measured for 100% POPC by an amount which is the sum of the perturbations due to the cationic and anionic species individually in binary mixtures (Marassi & Macdonald, 1992), according to eq 2:

$$(\Delta\nu_{+/-} - \Delta\nu_0) = (\Delta\nu_- - \Delta\nu_0) + (\Delta\nu_+ - \Delta\nu_0)$$
$$= m_+X_+ + m_-X_- \qquad (2)$$

For the case of GUVs composed of POPC + CHOL + POPG fusing with SUVs composed of DODAP + POPC + POPE, one expects no effect of either CHOL or POPE or POPC on the observed quadrupolar splittings other than through a dilution effect on the mole fractions of charged species.

The mole fraction of POPG in the GUVs decreases with increasing fusion due to a dilution effect which can be calculated according to eq 3:

$$X^{\mathrm{f}}_- = X^{\mathrm{i}}_- \left(1 + \frac{S}{G}\right)^{-1} \qquad (3)$$

where X^{f}_- and X^{i}_- are the mole fractions of POPG in the fused versus the initial GUVs, respectively, and (S/G) is the amount of SUV lipid fused per amount of GUV lipid present initially (i.e., the fused SUV/GUV lipid ratio).

In a similar fashion, one may calculate the manner in which the mole fraction of DODAP increases in the GUVs as a function of the amount of fused SUV lipid according to eq 4:

$$X^{\mathrm{f}}_+ = X^{\mathrm{SUV}}_+ \left(\frac{S}{G}\right)\left(1 + \frac{S}{G}\right)^{-1} \qquad (4)$$

where X^{SUV}_+ corresponds to the mole fraction of DODAP in the SUVs, while all other terms have been defined previously.

When eqs 3 and 4 are substituted into eq 2, one obtains eq 5, which allows one to predict the manner in which the quadrupolar splitting should change as a function of the extent of SUV fusion with GUVs, and how the prediction depends on the major variables:

$$(\Delta\nu_{+/-} - \Delta\nu_0) = \frac{(\Delta\nu_- - \Delta\nu_0) + m_+X^{\mathrm{SUV}}_+(S/G)}{1 + (S/G)} \qquad (5)$$

Alternatively, one may choose to extract the extent of fusion from the quadrupolar splitting data according to eq 6:

$$\frac{S}{G} = \frac{(\Delta\nu_{+/-} - \Delta\nu_0) - (\Delta\nu_- - \Delta\nu_0)}{m_+X^{\mathrm{SUV}}_+ - (\Delta\nu_{+/-} - \Delta\nu_0)} \qquad (6)$$

In both eqs 5 and 6, the quantity $\Delta\nu_-$ corresponds to the quadrupolar splitting measured prior to the addition of SUVs while $\Delta\nu_0$ corresponds to the quadrupolar splitting measured for 100% POPC. The percent fusion is then simply $[(S/G)^{\mathrm{fused}}/(S/G)^{\mathrm{global}}] \times 100$.

Figure 7 illustrates the manner in which the quadrupolar splitting for POPC-α-d_2 is predicted to change as a function of (S/G), i.e., the amount of fused SUV lipid per GUV lipid, for two types of SUVs fusing with two types of GUVs. The SUVs were assumed to consist of DODAP + POPC either 50/50 or 90/10. The GUVs were assumed to consist of POPC + CHOL + POPG either 60/30/10 or 69/30/1. The greatest change in the quadrupolar splitting results from the fusion of the SUVs containing the greatest amount of DODAP with the GUVs containing the greatest amount of POPG. Similar predictive curves may be produced for any

Table 4: Quantification of Fusion from Experimental ^{2}H NMR Quadrupolar Splittings[a]

vesicle lipid composition	global SUV/GUV lipid ratio	fused SUV/GUV lipid ratio	fused DODAP/POPG lipid ratio	% fusion	SUVs fused per GUV
GUV POPC/CHOL/POPG (60/30/10) + SUV DODAP/POPC (50/50)	0	0	0	0	0
	0.174	0.064	0.322	37	9
	0.347	0.172	0.862	50	22
	0.521	0.304	1.52	58	39
	0.695	0.451	2.25	65	58
GUV POPC/CHOL/POPG (70/20/10) + SUV DODAP/POPC (50/50)	0	0	0	0	0
	0.203	0.065	0.323	32	4
	0.405	0.185	0.924	46	13
	0.608	0.291	1.45	48	20
	0.812	0.399	2.00	49	27
GUV POPC/CHOL/POPG (69/30/1) + SUV DODAP/POPC (50/50)	0	0	0	0	0
	0.200	0.013	0.684	7	< 1
	0.400	0.043	2.15	11	2
	0.600	0.114	5.68	19	4
	1.00	0.214	10.7	21	8
GUV POPC/CHOL/POPG (60/30/10) + SUV DODAP/POPC/POPE (40/40/20)	0	0	0	0	0
	0.109	0.109	0.434	100	14
	0.217	0.217	0.870	100	29
	0.326	0.326	1.30	100	41
	0.434	0.380	1.52	87	49
	0.543	0.455	1.82	84	58
	0.651	0.594	2.20	84	71

[a] Quantification was carried out according to eq 5 in the text.

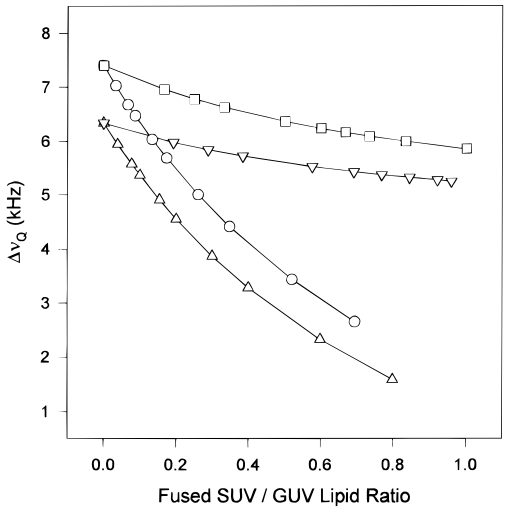

FIGURE 7: Predicted dependence of the quadrupolar splitting from POPC-α-d_2 incorporated into GUVs as a function of fused SUVs for different GUV and SUV compositions. Quadrupolar splittings were calculated according to eq 5 as described in the text. Squares: GUVs = POPC + CHOL + POPG (60/30/10), SUVs = DODAP + POPC (90/10). Circles: GUVs = POPC + CHOL + POPG (60/30/10), SUVs = DODAP + POPC (50/50). Inverted triangles: GUVs = POPC + CHOL + POPG (69/30/1), SUVs = DODAP + POPC (90/10). Triangles: GUVs = POPC + CHOL + POPG (69/30/1), SUVs = DODAP + POPC (50/50).

combination of SUVs plus GUVs, or for any choline deutero-labeling position, using eq 5 provided independent calibration data for the corresponding binary mixtures are available. We note as well that the quadrupolar splittings measured in MLVs composed of corresponding mixtures of lipids agree closely with the predictions of eq 5.

The extent of fusion associated with the various GUV and SUV systems studied was extracted from the experimental quadrupolar splitting data according to eq 6 and is tabulated in Table 4. Details for all cases studied here are listed, with the exception of that in which SUVs were added to GUVs of composition POPC + CHOL (70/30). As discussed previously, no fusion was exhibited in this instance. In Figure 5, where the experimental quadrupolar splitting data are plotted versus the global SUV/GUV lipid ratio for the various vesicle mixing cases, the solid lines represent the percent fusion according to eq 6, averaged over a particular data range, and then employed to predict the quadrupolar splitting according to eq 5. For instance, in the case of POPE-containing SUVs, eq 6 indicates that virtually 100% fusion is achieved until the DODAP/POPG ratio exceeds 1:1, after which further additions of SUVs produce only approximately 85% fusion. In contrast, GUVs lacking POPG fail completely to fuse with SUVs containing DODAP but no POPE. When just 1 mol % POPG is present in the GUVs, about 20% fusion is achieved upon adding SUVs composed of DODAP + POPC (50/50), but only after an initial lag during which only about 10% of the added SUVs fuse. For the case of GUVs containing 10 mol % POPG, levels of fusion approach 55%, but again only after an initial lag.

These analyses of the ^{2}H NMR data confirm quantitatively the conclusions drawn previously concerning the facts that considerable fusion occurs even for rather low levels of complementary charge on the GUVs, that increasing the level of complementary charge enhances fusion, and that a further enhancement to 100% fusion occurs when POPE is present even in rather low amounts.

The ^{2}H NMR quadrupolar splittings may be interpreted further to reveal the number of SUVs fusing per GUV, provided certain judicious assumptions are made regarding the size of the two types of vesicles. Specifically, the quantity (*S/G*) in eqs 5 and 6 may be replaced as

$$S/G = \left(\frac{N_{SUV}}{N_{GUV}}\right)\left(\frac{L_{SUV}}{L_{GUV}}\right) \qquad (7)$$

where N_{SUV}/N_{GUV} is the number of SUVs fusing per GUV, while L_{SUV} and L_{GUV} are number of lipids per SUV and GUV,

respectively. The latter quantities may be calculated for a given size of SUV or GUV from the known cross-sectional areas of the lipid species involved.

Table 4 lists the results obtained when this analysis is performed for the cases investigated here. In these calculations, the surface area occupied by CHOL was taken to equal 50 Å^2, whereas the surface areas for POPC, POPG, and DODAP were all taken to be 68 Å^2 (Altenbach & Seelig, 1984; Yeagle, 1988). Previous freeze-fracture electron microscopy and quasi-elastic light scattering measurements on the GUVs produced in our laboratory indicate that GUVs composed of POPC + CHOL + POPG (60/30/10) have an average diameter on the order of 800 nm (Marassi *et al.*, 1993). The factors critical to producing this rather large diameter appear to be the presence of both cholesterol, for mechanical stability, and POPG, for electrostatic swelling. GUVs composed of POPC + CHOL (70/30), for instance, had diameters on the order of 450 nm (Marassi *et al.*, 1993). For the purposes of eqs 3 and 4, we chose to employ diameters of 800, 600 and 450 nm for GUVs composed of POPC + CHOL + POPG 60/30/10, 70/20/10, and 69/30/1, respectively. For sonicated SUVs composed of mixtures of DODAP + POPC, we used the diameter of approximately 75 nm reported by Wrobel and Collins (1995) for nearly identical situations.

CONCLUDING REMARKS

The ^{2}H NMR results reported here demonstrate the utility of this technique for detecting and quantifying fusion of asymmetric lipid vesicles. It has proved possible to measure the effects of several factors known to favor fusion, including complementary charge and the presence of PE. An important application of this technology will be to characterize the fate of vesicle contents post-fusion. A specific example of some immediate relevance is the question of the fate of DNA in DNA + cationic amphiphile packages such as those employed in transfection technologies.

ACKNOWLEDGMENT

We thank Peter Mitrakos for his adept synthesis of DODAP.

REFERENCES

Akutsu, H., & Seelig, J. (1981) *Biochemistry 20*, 7366−7337.
Allen, T. M., Hong, K., & Papahadjopoulos, D. (1990) *Biochemistry 29*, 2976−2985.
Aloy, M. M., & Rabout, C. (1913) *Bull. Soc. Chim. Fr. 13*, 457−460.
Altenbach, C., & Seelig, J. (1984) *Biochemistry 23*, 3913−3920.
Aneja, R., Chada, J. S., & Davies, A. P. (1970) *Biochim. Biophys. Acta 218*, 102−111.
Bailey, A. L., & Cullis, P. R. (1994) *Biochemistry 33*, 12573−12580.
Bloom, M., Burnell, E. E., Valic, M. I., & Weeks, G. (1975) *Chem. Phys. Lipids 14*, 107−112.
Cullis, P. R., & De Kruijff, B. (1979) *Biochim. Biophys. Acta 559*, 399−420.
Davis, J. H., Jeffrey, K. R., Bloom, M., Valic, M. I., & Higgs, T. P. (1976) *Chem. Phys. Lett. 42*, 390−394.
Düzgüneş, N., Goldstein, J. A., Friend, D. S., & Felgner, P. L. (1989) *Biochemistry 28*, 9179−9184.
Ellens, H., Bentz, J., & Szoka, F. C. (1985) *Biochemistry 24*, 3099−3106.
Ellens, H., Siegel, D. P., Alford, D., Yeagle, P. L., Boni, L., Lis, L. J., Quinn, P. J., & Bentz, J. (1989) *Biochemistry 28*, 3692−3703.
Felgner, P. L., Gadek, T. R., Holm, M., Roman, R., Chan, H. W., Wenz, M., Northrop, J. P., Ringold, G. M., & Danielsen, M. (1987) *Proc. Natl. Acad. Sci. U.S.A. 84*, 7413−7417.
Friend, D. S., Papahadjopoulos, D., & Debs, R. J. (1996) *Biochim. Biophys. Acta 1278*, 41−50.
Gustafsson, J., Arvidson, G., Karlsson, G., & Almgren, M. (1995) *Biochim. Biophys. Acta 1235*, 305−312.
Harbison, G. S., & Griffin, R. G. (1984) *J. Lipid Res. 25*, 1140−1142.
Helm, C. A., Israelachvili, J. N., & McGuiggan, P. M. (1992) *Biochemistry 31*, 1794−1805.
Hoekstra, D. (1990) *J. Bioenerg. Biomembr. 22*, 121−125.
Leventis, R., & Silvius, J. R. (1990) *Biochim. Biophys. Acta 1023*, 124−132.
Litzinger, D. C., & Huang, L. (1992) *Biochim. Biophys. Acta 1113*, 201−227.
Macdonald, P. M., Liesen, J., & Marassi, F. M. (1991) *Biochemistry 30*, 3558−3566.
Marassi, F. M., & Macdonald, P. M. (1992) *Biochemistry 31*, 10031−10036.
Marassi, F. M., Shivers, R. R., & Macdonald, P. M. (1993) *Biochemistry 32*, 9936−9943.
Mitrakos, P., & Macdonald, P. M. (1996) *Biochemistry 35*, 16714−16722.
Nir, L., Düzgüneş, N., & Bentz, J. (1983) *Biochim. Biophys. Acta 735*, 160−172.
Portis, A., Newton, C., Pangborn, W., & Papahadjopoulos, D. (1979) *Biochemistry 18*, 780−790.
Rance, M., & Byrd, R. A. (*1983) J. Magn. Reson. 52*, 221−240.
Scherer, P. G., & Seelig, J. (1989) *Biochemistry* 28, 7720−7728.
Seelig, J. (1978) *Biochim. Biophys. Acta 515*, 105−140.
Seelig, J., & Macdonald, P. M. (1987) *Acc. Chem. Res. 20*, 221−228.
Seelig, J., Macdonald, P. M., & Scherer, P. G. (1987) *Biochemistry 26*, 7535−7541.
Stamatatos, L., Leventis, R., & Silvius, J. R. (1988) *Biochemistry 27*, 3917−3925.
Struck, D., Hoekstra, D., & Pagano, R. E. (1981) *Biochemistry 20*, 4093−4099.
White, J. M. (1992) *Science 258*, 917−924.
Wilschut, J., & Hoekstra, D., Eds. (1993) *Membrane Fusion*, CRC Press, Boca Raton, FL.
Wilschut, J., Düzgüneş, N., Fraley, R., & Papahadjopoulos, D. (1980) *Biochemistry 19*, 6011−6021.
Wrobel, I., & Collins, D. (1995) *Biochim. Biophys. Acta 1235*, 296−304.
Yeagle, P. (1988) *Biology of Cholesterol*, CRC Press, Boca Raton, FL.
Zhou, X., & Huang, L. (1994) *Biochim. Biophys. Acta 1189*, 195−203.

BI9621270